Research Paper
Computational Methods for Differential Equations
http://cmde.tabrizu.ac.ir
Vol. *, No. *, *, pp. 1-17
DOI:10.22034/cmde.2026.66792.3156

An artificial neural network scheme for the numerical analysis of a Zika virus model with the effect of environmental pollution

Muhammad Waseem* **and Maryam Nusrat**

Department of Mathematics, COMSATS University Islamabad, Vehari Campus, Pakistan.

Abstract

The objective of this study is to present numerical computations of a fractional-order Zika virus (ZIKV) model by developing a computational framework that incorporates stochastic Levenberg-Marquardt backpropagation neural networks (LMBNNs). In this paper, we present a fractional-order model for the ZIKV with the effect of environmental pollution, utilizing the Caputo fractional derivative. Fractional-order derivatives have been employed to achieve more precise performance of the fractional-order mathematical ZIKV model in comparison to integer-order derivatives. The fractional order ZIKV model is categorized into five classes: susceptible (S_h), stressed (S_{h_s}), infected (I_h), susceptible (S_v) and infected (I_v). Four different cases involving fractional order derivatives have been numerically demonstrated using the mathematical ZIKV model. The results obtained from the ZIKV model are displayed by employing the computational stochastic framework of LMBNNs, which involves verification, training, and evaluation procedures aimed at reducing the mean square error (MSE). For the fractional-order mathematical ZIKV model, the data selection process is carried out as follows: 70% for training and 15% for certification and testing. A thorough study has been conducted to examine regression analysis, correlation, MSE, error histograms (EHs), and information about STs in order to evaluate the proficiency and accuracy of the suggested computing framework. The numerical findings shows the validity of the stochastic LMBNNs computing framework.

Uncorrected

Keywords. Artificial neural networks, Caputo fractional derivative, Levenberg-Marquardt backpropagation, Numerical simulations.

1991 Mathematics Subject Classification. 68T07, 68T20, 92B20.

1. Introduction

For humans, mosquito-borne disease epidemics are a major global health issue. The transmission rate of many viruses such as dengue, coronavirus, influenza, and other human infections have transmitted around the world in recent years. One of the diseases caused by vectors, the ZIKV, is spread to people by the bite of an infected Aedes genus mosquito [12]. ZIKV is classified as part of the Flaviviridae family of flaviviruses [53]. Mosquitoes are the cause of spreading diseases to humans through their bites. Even the virus can also spread via sexual interaction, blood donations, and pregnancy from a pregnant woman to her fetus [31]. The symptoms of that disease involve fever, irritation, conjunctivitis, muscle and joint discomfort, headaches, and malaise. Most ZIKV patients have no symptoms at all or mild symptoms and do not need to be hospitalized. As of yet, there is no approved medication or vaccination for ZIKV. The ZIKV first appeared in a Rhesus monkey in Uganda's Zika jungle in 1947 [1]. First cases of humans were found in Nigeria in 1954, and after that time, sporadic human cases have been described on occasion [1, 29]. There are several outbreaks of ZIKV occurring all over the world, including in Brazil, Venezuela, Honduras, Canada, and El Salvador. Between 440,000 and 1,500,000 confirmed probable cases, Brazil has the highest number of ZIKV cases ever reported [11, 45]. In 2016, the World Health Organization labeled ZIKV an epidemic because of microcephaly clustering and neurological disorders in several virus-affected locations, such as Brazil. ZIKV has the potential to be transmitted across the globe, so it's crucial to investigate the disease's transmission patterns.

Received: 15 April 2025; Accepted: 07 November 2026.
∗ Corresponding author. Email: mwaseem1889@gmail.com.

It has been recognized that mathematical models are crucial tools for examining the dynamics of disease spreading. The ZIKV continued to propagate to other regions, with 86 countries having reported cases of infection to date. We may establish control techniques to take over the disease by employing mathematical modeling to identify the critical parameters involved in the disease's advancement. Many mathematical models have been presented to show the different levels of complexity depending on the characteristics of the problem; for example, some systems require a higher level of complexity to simulate, particularly those that are stiff and intricate. There is a long history of mathematical modeling offering insights into the control and spread of many viral diseases worldwide [4, 17, 19, 30, 43, 44]. Another significant issue facing contemporary society is pollution of the environment. There has been an exponential rise in environmental contamination in the recent past. The environment suffers greatly as a result of increased motor vehicle use, industrialization, and construction projects. Continuous exposure to environmental pollution is leading to numerous diseases and disabilities. Infections and disease transmission may be facilitated by environmental pollution, according to several studies [9, 27]. Mathematical models have also been used to address how pollution contributes to the spread of infectious diseases [5, 18, 47].

The review by Wiratsudakul et al. [54] intends to give a general overview of mathematical modeling techniques, especially those that were devised for the transmission of the ZIKV. They explored the use of mathematical frameworks for estimating Zika import risk and establishing interventions, and they gave a demonstration of how the models were used during the Zika epidemics. Suparit et al. [51] used data from the 2015–2016 Zika epidemics in Bahia, Brazil, to develop a mosquito-borne compartmental model that corresponds to the virus's potential future spread and assessed the effectiveness of vector control measures. A mathematical model of the ZIKV on a complex network was developed by Srivastav et al. [49], with consideration for both mosquito-borne and sexually transmitted forms of the disease. Rahman et al. [36] devised an algorithm to determine the parameters that can be inferred from the given data, employing a mathematical framework of ZIKV dynamics and a complex-step derivation estimate. A deterministic Zika model, which included vector control, human awareness, and sexual and vector transmission channels in the depletion of disease-induced mortality, was established and evaluated by Biswas et al. [10]. Goswami and Shanmukha [16] gave a mathematical model by incorporating standard incidence-type interactions for the spread of the ZIKV from human to human. Taylor [52] developed a novel mathematical approach for ZIKV interactions that involves four control measures, comprising two preventive measures for mosquito bites and sexual transmission. Sharma et al. [48] devised a compartmental model, with the objective of studying how vaccinations affect disease control by providing the best feasible outcome. Alzahrani et al. [8] established a unique mathematical model that incorporated ZIKV mutations along with three controls to demonstrate their findings. An innovative ZIKV model was formulated by Ali et al. [3] that incorporates human cognition in the host population as well as mosquito and mosquito-borne transmission. Alshehri and Hajji [6] proposed an effective mathematical model for explaining ZIKV spread with a nonlinear general incidence rate. A compartmental model was presented by Kumar et al. [26] to examine the Zika outbreak in Brazil. Sabir et al. [39] developed a swarming computational method to simulate the spread of ZIKV across the susceptible, exposed, infected, and recovered categories. To explain the risk of virus transmission by immigrants, Yue et al. [55] developed a ZIKV model involving immigrants. They presented screening strategies for immigrants to determine the best control scheme based on an optimal control approach and cost analysis, emphasizing the potential for suitable screening in ZIKV management. Murugappan et al. [32] studied a population of males, females, and children utilizing a non-linear mathematical model of ZIKV transmission. A new deterministic mathematical model was presented by Omede et al. [34] to study the dynamics of co-infection between the ZIKV and HIV, considering both horizontal as well as vertical transmission. Using a probabilistic neural network-based intelligent computation solution, Suantai et al. [50] provided the computational outcomes and perspectives of the SEIR framework employing the Zika virus propagation. Huo et al. [20] constructed a novel model for the transmission of the ZIKV, which comprises three modes of transmission: vertical transmission, sexual transmission between males and females, and human transmission through mosquito bites. Jose et al. [23] studied the epidemic dynamics of dengue fever (DF) and ZIKV co-infections using a mathematical model. An innovative mathematical model was devised by Zafar et al. [56] to investigate the dynamics of ZIKV infections with the mutant in actual, reported cases in Colombia.

Ahmadkhanpour et al. [2] presented a unique method termed improved back-propagation that uses artificial neural networks to solve ordinary differential equations. Multilayer perceptron neural networks, which have adjustable

Uncorrected Proof

parameters like weights and biases, were employed. Dadashzadeh et al. [13] introduced the flexible fractional wavelet neural network, a unique neural network architecture that adds two more fractional wavelet parameters to conventional wavelet networks. The suggested method was assessed for both one-dimensional and multi-dimensional dynamic system identification. The accuracy and efficiency of the network are shown to be greatly enhanced by the fractional wavelet parameters. In order to solve partial differential equations, Liu et al. [28] employed a physically informed neural network and adaptive activation function tuning. They also introduced several nonlinear Schrödinger equations that are relevant to semiconductor optical amplifier fiber laser applications.

It is better to use fractional order derivatives rather than integer order models to comprehend the dynamics of Zika virus transmission. While using the fractional order derivative one may obtain significantly better analysis, forecasting, and estimation of illness parameters of ZIKV than implemented with the help of a conventional one. Fractional derivatives have the advantage of offering more degrees of freedom, which enables a wider variety of analysis of the dynamic behavior of the system, including nonlocal solutions. Among the many fractional derivatives found in the literature, one of the most popular methods in fractional calculus is the Caputo fractional derivative. One major advantage of using the Caputo fractional derivative is that it preserves the same initial conditions as conventional derivatives.

Research on fractional-order differential equations (FDEs) is crucial across various fields, including mathematics, physics, control systems, and particularly engineering. In many distinct regions, fractional calculus is a practical mathematical tool for comprehending and solving real-world issues [7, 21, 22]. By using fractional operators, khan et al. [24] used artificial intelligence and neural networking techniques to mimic the dynamics of Zika virus transmissions between hums and mosquitoes. In order to comprehend the long-term consequences of public health issues, they demonstrated how fractional derivatives allow for a more thorough description of memory effects and time delays in the disease transmission processes. In the context of Zika virus transmission, they demonstrated, this is especially important because accurate forecasts of outbreak trajectories require assuming delays in infection onset and variance in transmission rates.

A stochastic numerical strategy was presented by Sabir et al. [41] to address a fractional order water pollution problem model by applying artificial neural networks and the Levenberg-Marquardt backpropagation method. Rezapour et al. [38] devised a novel mathematical model that employs the fractional-order Caputo differential to illustrate how the ZIKV transmits from humans to mosquitoes. A Caputo fractional-order-based SEIR framework for hosts and an SEI framework for mosquitoes were established by Prasad et al. [35] to examine ZIKV transmission. They inspected the outbreaks that occurred between 2013 and 2016 in six of the main French Polynesia archipelagos. Sabir et al. [42] provided a computational framework employing stochastic L-MBNNs to simulate the fractional-order computational influenza disease model. The influenza disease nonlinear system (IDNS) was numerically simulated by Sabir et al. [40] employing stochastic artificial neural networks (ANNs) processes backed by LMB, or ANNs-LMB. To solve the six distinct IDNS variations, numerical computations were carried out using the stochastic ANNs-LMB. This work highlights several innovative points, including:

- A fractional-order ZIKV model formulation is explained and effectively solved numerically.
- Further precise solutions for the fractional order ZIKV model have been generated by applying the Caputo fractional order derivatives.
- To illustrate the numerical representations of the mathematical ZIKV model, four fractional-order derivative cases have been investigated. The fractional-order derivatives are considered to lie between 0 and 1.
- The goal of developing the computational stochastic structure relying on LMBNNs is to numerically address fractional-order problems.
- The consistency and reliability of the proposed LMBNNs are assessed through EHs, correlation, STs, MSE, and regression analysis to slove fractional order mathematical ZIKV model.

We applied the Caputo fractional derivative to give a mathematical model of Zika virus propagation [26]. In the procedure of modeling, the classification of human population into three separate categories: susceptible (S_h), stressed (S_{h_s}), and infected (I_h). During the formulation process, the human susceptible population is classified into stressed compartment. Similarly, we divided the population of mosquito into two categories: susceptible (S_v) and infected (I_v). The flow chart of the mathematical ZIKV model is shown in Figure 1.

Uncorrected Proof

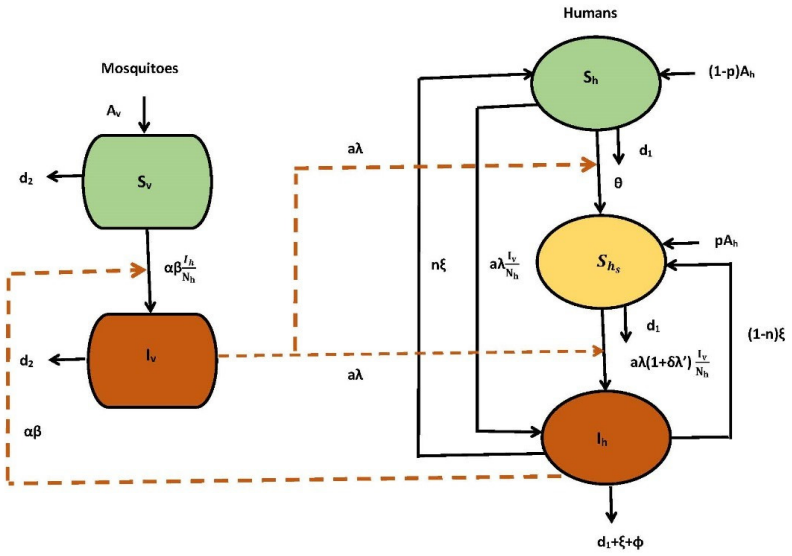


FIGURE 1. Schematic diagram of ZIKV model.

The ZIKV model [26] in its general form is provided in the form of system of differential equations as

$$\begin{aligned}
\frac{dS_h}{dt} &= (1-p)A_h - a\lambda S_h\frac{I_v}{N_h} - \theta S_h + n\xi I_h - d_1 S_h,\\
\frac{dS_{h_s}}{dt} &= pA_h - a\lambda(1+\delta\lambda^{'})S_{h_s}\frac{I_v}{N_h} + \theta S_h + (1-n)\xi\ I_h - d_1 S_{h_s},\\
\frac{dI_h}{dt} &= a\lambda S_h\frac{I_v}{N_h} + a\lambda(1+\ \delta\lambda^{'})S_{h_s}\frac{I_v}{N_h} - (d_1+\phi+\xi)I_h,\\
\frac{dS_v}{dt} &= A_v - a\beta S_v\frac{I_h}{N_h} - d_2\ S_v,\\
\frac{dI_v}{dt} &= a\beta S_v\frac{I_h}{N_h} - d_2 I_v.
\end{aligned} \tag{1.1}$$

We have considered the following initial conditions:

$$S_h(0)\geq 0, S_{h_s}(0)\geq 0,\ I_h(0)\geq 0, S_v(0)\geq 0, I_v(0)\geq 0. \tag{1.2}$$

Table 1 displays the description of the state variables for each category according to the nonlinear ZIKV model.

The rest parts of the article are explained as follows: The ZIKV model, a fractional-order mathematical model, is designed and given in Section 2. Section 3 provides a description of the stochastic framework relying on the LMBNNs. Section 4 includes the simulations and results generated for the fractional order ZIKV model using the suggested approach. The concluding remarks of this article are presented in Section 5.

2. Design of the fractional order ZIKV model

The study of fractional calculus (FC) was introduced centuries ago during Newton's time, but it has gained considerable importance in recent decades. Fractional-order derivatives have been found to produce a better fit between

Uncorrected

TABLE 1. Description of the state variables for each category of the ZIKV model.

Description	Notation
Population's constant rate of human recruitment	A_h
Population's constant rate of mosquito recruitment	A_v
Proportion of the new population enters the S_{h_s} compartment	p
Remaining proportion belongs to the S_h class	$(1-p)$
Constant rate of access of the susceptible population into the stressed compartment	θ
Proportion of the recovered group goes into the S_{h_s} class	$(1-n)$
Fraction of the class joins the S_h compartment	n
Human population's natural death rate	d_1
Human population's disease-related death rate	ϕ
Human population's rate of recovery	ξ
Biting rate of mosquito	a
Probability of one infectious mosquito spreading the disease to a susceptible human per bite	λ
Possibility of transmission from an infected person to a vulnerable mosquito via every bite	β
Mosquito's natural rate of death	d_2
Stress level	δ
Rate to which stress raises λ	$\lambda^{'}$
Overall populations of humans	N_h
Overall populations of mosquitoes	N_v

Uncorrected Proof

simulated and real data than do conventional models that employ integer-order derivatives [14, 15]. Moreover, the fractional-order (FO) derivatives have been used to get analytical or numerical findings derived from nonlinear differential models. The goal of this research is to demonstrate the value and significance of the fractional order ZIKV model based on the AI processes together with the LMBNNs. As $N_h = S_h + S_{h_s} + I_h$, and, $N_v = S_v + I_v$, $A_v = N_v d_2$ and $A_h = N_h d_1$. Both the human and mosquito populations are non-dimensionalized in order to minimize the system's (1.1) parameter number by $x_1 = \frac{S_h}{N_h}$, $x_2 = \frac{S_{h_s}}{N_h}$, $i_h = \frac{I_h}{N_h}$, $x_3 = \frac{S_v}{N_v}$, $i_v = \frac{I_v}{N_v}$ and $m = \frac{\frac{A_v}{d_2}}{N_h}$. The variables S_h, S_{h_s} , I_h, S_v, and I_v will be interpreted as x_1, x_2, i_h, x_3, and i_v. The class of humans who are under the effect of stress is represented by S_{h_s}, susceptible humans are symbolized by S_h, and infected humans are represented by I_h. Likewise, the susceptible mosquito is denoted as S_v, while the infected mosquito is denoted as I_v.

Now we will extend ZIKV model (1.1) using the fractional derivative, as

$$\begin{aligned}
D_t^\alpha S_h &= (1-p)d_1 - a\lambda m S_h I_v - \theta S_h + n\xi I_h - d_1 S_h,\\
D_t^\alpha S_{h_s} &= pd_1 + \theta S_h - a\lambda(1+\delta\lambda^{'})mS_{h_s} I_v + (1-n)\xi I_h - d_1 S_{h_s},\\
D_t^\alpha I_h &= a\lambda m S_h I_v + a\lambda m(1+\delta\lambda^{'})S_{h_s} I_v - (d_1+\phi+\xi)I_h,\\
D_t^\alpha S_v &= d_2 - a\beta S_v I_h - d_2 S_v,\\
D_t^\alpha I_v &= a\beta S_v I_h - d_2 I_v,
\end{aligned} \tag{2.1}$$

subject to initial conditions $S_h(0) \geq 0$, $S_{h_s}(0) \geq 0$, $I_h(0) \geq 0$, $S_v(0) \geq 0$, $I_v(0) \geq 0$.

Where α represents the FO derivative defined in the Caputo sense, which is utilized to represent the fractional order ZIKV model in system (2.1). The fractional-order derivatives are considered to lie between 0 and 1. However, in order to solve the nonlinear ZIKV model with more realistic results, these derivatives are employed in this study.

3. Designed stochastic framework: LMBNNs

This section describes the proposed LMBNN structure to solve all variants of the fractional order ZIKV model. Figure 2 illustrates the step-by-step workflow using a computational stochastic approach for tackling the fractional order ZIKV model. The model is illustrated in the first part of Figure 2, and the system's mathematical representations are presented in the second part. The third part outlines the LMBNNs'methodological steps, while the last part

TABLE 2. Configuring the LMBNNs execution parameters.

Index	Setting
Fitness objective (MSE)	0
Iteration	1000
Adaptive parameter (mu)	0.001
Maximum value of (mu)	10^{-6}
Hidden neurons	10
Validation trials	15%
Samples for testing and vefification	15%
Samples for training	70%
Sample choice	Arbitrary
Solver for dataset generation	Adam method
Input, output and hidden layers	Single for all three
Adams solver parameter for stopping and execution	Default

describes the simulations of the outcomes. Figure 3(A) shows the structure of the multi-layer network of neurons, and Figure 3(B) hidden neurons, one input vector, and five target vectors. Table 2 displays the parameter configuration for the ZIKV model based on the stochastic structure. Furthermore, the references contain the execution process as well as some crucial theoretical information based on the LMB algorithms [25, 33, 37, 46].

4. Discussion-based simulations and investigation

This section provides the numerical computations of ZIKV model (2.1) in four distinct variations through the creation of a computational framework that incorporates stochastic procedure of artificial neural networks with Levenberg-Marquardt backpropagation (LMBNNs). The numerical results based on the fractional order mathematical ZIKV model (2.1) with Caputo fractional derivative are displayed by selecting the different values of FO $\alpha = 0.7, 0.8, 0.9$ and $\alpha = 0.95$. In the subsequent cases, the differential description for each variant is presented as follows:

Case 1. Assume the fractional order ZIKV model is shown as:

$$\begin{aligned}
D_t^{0.7} S_h &= (1-p)d_1 - a\lambda m S_h I_v - \theta S_h + n\xi I_h - d_1 S_h, \quad S_h(0) = 100,\\
D_t^{0.7} S_{h_s} &= pd_1 + \theta S_h - a\lambda(1+\delta\lambda^{'}) m S_{h_s} I_v + (1-n)\xi I_h - d_1 S_{h_s}, \quad S_{h_s}(0) = 70,\\
D_t^{0.7} I_h &= a\lambda m S_h I_v + a\lambda m(1+\delta\lambda^{'}) S_{h_s} I_v - (d_1+\phi+\xi) I_h, \quad I_h(0) = 20,\\
D_t^{0.7} S_v &= d_2 - a\beta S_v I_h - d_2 S_v, \quad S_v(0) = 80,\\
D_t^{0.7} I_v &= a\beta S_v I_h - d_2 I_v, \quad I_v(0) = 30.
\end{aligned} \tag{4.1}$$

Case 2. Assume the fractional order ZIKV model is given as:

$$\begin{aligned}
D_t^{0.8} S_h &= (1-p)d_1 - a\lambda m S_h I_v - \theta S_h + n\xi I_h - d_1 S_h, \quad S_h(0) = 100,\\
D_t^{0.8} S_{h_s} &= pd_1 + \theta S_h - a\lambda(1+\delta\lambda^{'}) m S_{h_s} I_v + (1-n)\xi I_h - d_1 S_{h_s}, \quad S_{h_s}(0) = 70,\\
D_t^{0.8} I_h &= a\lambda m S_h I_v + a\lambda m(1+\delta\lambda^{'}) S_{h_s} I_v - (d_1+\phi+\xi) I_h, \quad I_h(0) = 20,\\
D_t^{0.8} S_v &= d_2 - a\beta S_v I_h - d_2 S_v, \quad S_v(0) = 80,\\
D_t^{0.8} I_v &= a\beta S_v I_h - d_2 I_v, \quad I_v(0) = 30.
\end{aligned} \tag{4.2}$$

Case 3. Assume the fractional order ZIKV model is displayed as:

Uncorrected Proof

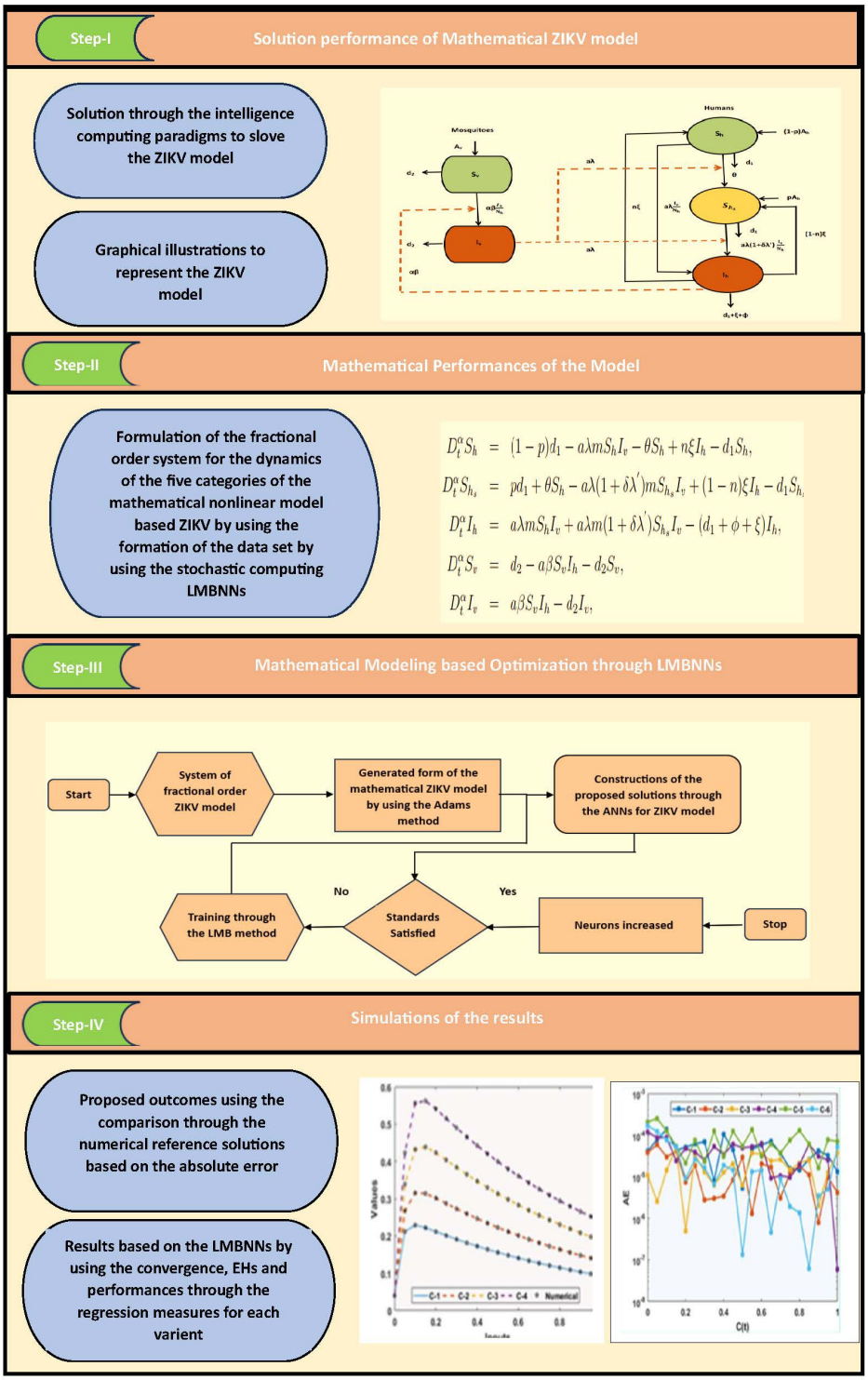
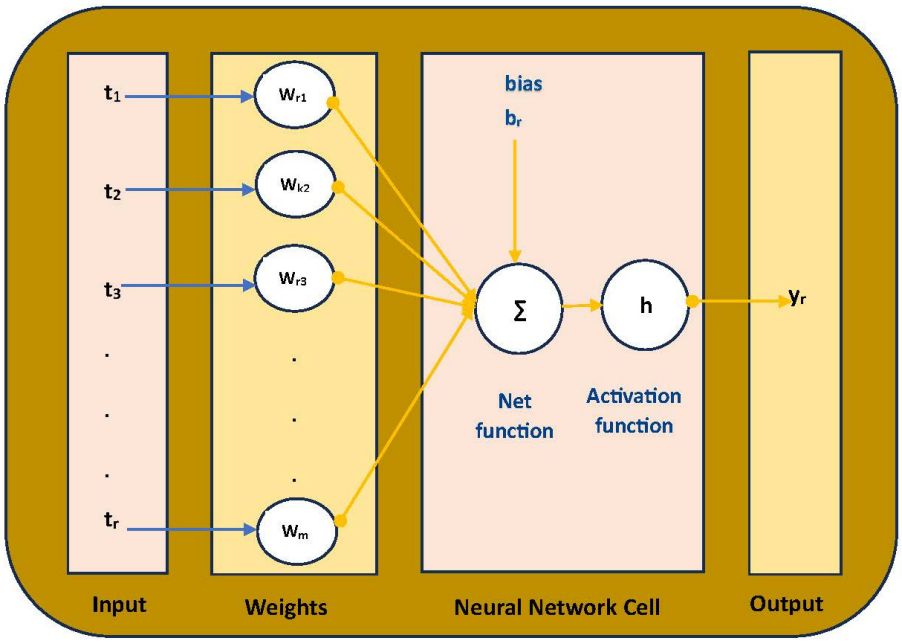
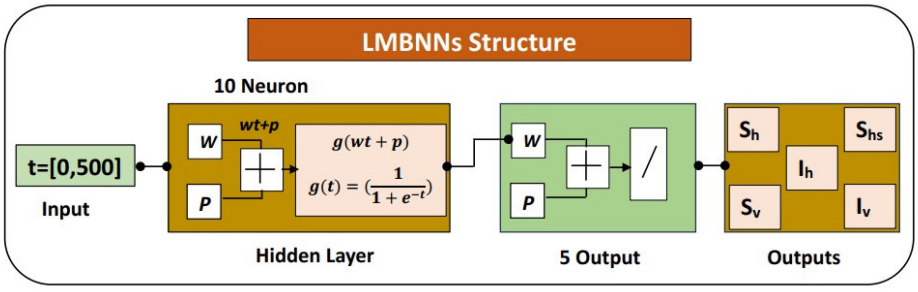


FIGURE 2. Graphical representations of constructed LMBNNs to solve the fractional order ZIKV model: Phase 1 presents a review of the problem. Phase 2 is an illustration of the mathematical system. Phase 3 employs the LMBNNs to identify the practical block. The simulation results and analysis are shown in Phase 4.



(A) Construction of general form of single neuron.

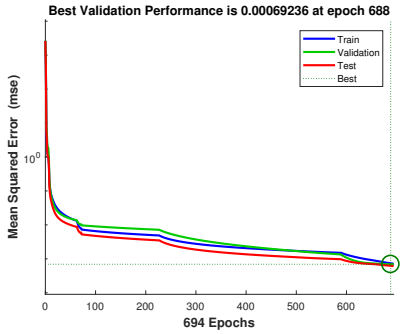


(B) Proposed layer structure, a single vector based input layer, 10 hidden neurons in hidden layer, and five outcome vectors in output layer.

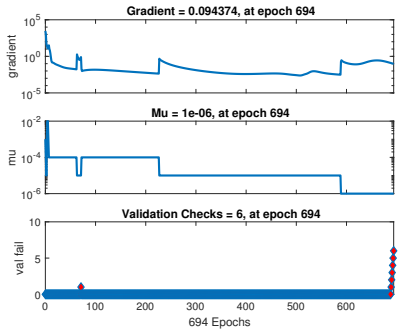
FIGURE 3. Stochastic structure of LMBNNs for sloving the ZIKV model.

$$
\begin{aligned}
D_t^{0.9} S_h &= (1-p)d_1 - a\lambda m S_h I_v - \theta S_h + n\xi I_h - d_1 S_h, \quad S_h(0) = 100,\\
D_t^{0.9} S_{h_s} &= pd_1 + \theta S_h - a\lambda(1+\delta\lambda^{'}) m S_{h_s} I_v + (1-n)\xi I_h - d_1 S_{h_s}, \quad S_{h_s}(0) = 70,\\
D_t^{0.9} I_h &= a\lambda m S_h I_v + a\lambda m(1+\delta\lambda^{'}) S_{h_s} I_v - (d_1 + \phi + \xi) I_h, \quad I_h(0) = 20,\\
D_t^{0.9} S_v &= d_2 - a\beta S_v I_h - d_2 S_v, \quad S_v(0) = 80,\\
D_t^{0.9} I_v &= a\beta S_v I_h - d_2 I_v, \quad I_v(0) = 30.
\end{aligned}
\tag{4.3}
$$

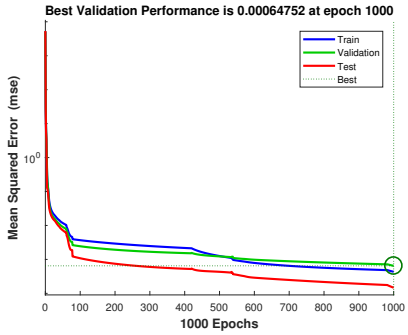
Case 4. Assume the fractional order ZIKV model is written as:



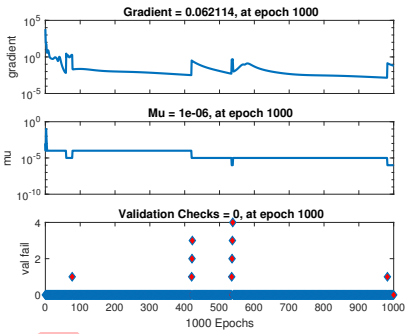
(A) MSE(1).



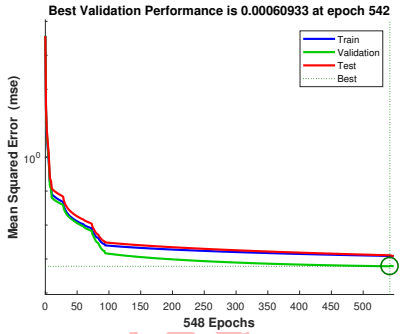
(B) STs(1).



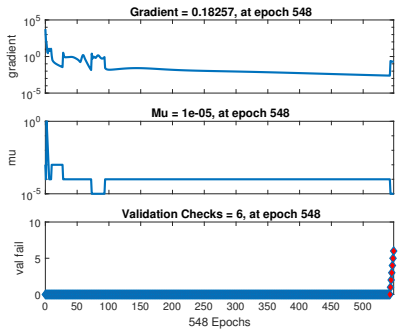
(C) MSE(2).



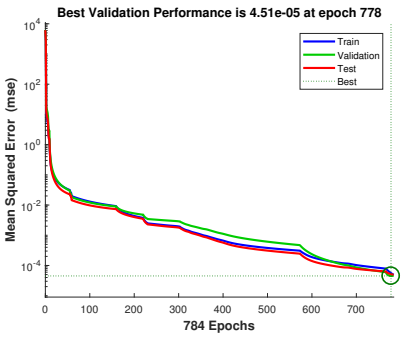
(D) STs(2).



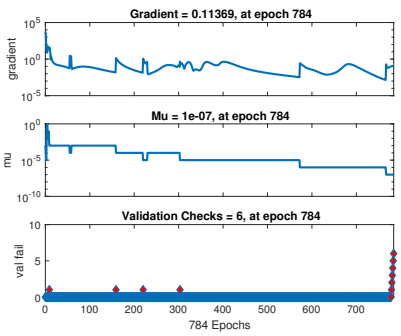
(E) MSE(3).



(F) STs(3).

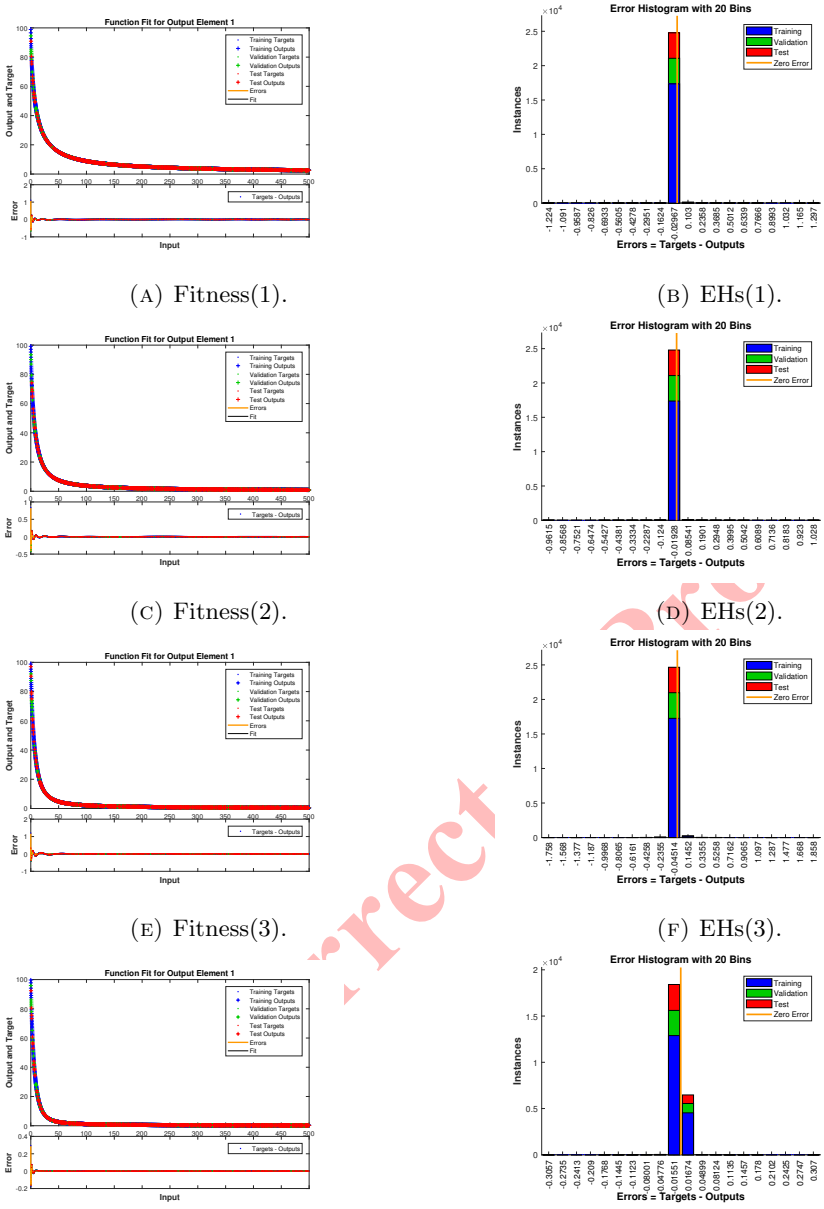


(G) MSE(4).



(H) STs(4).

FIGURE 4. Performances of STs and MSE for solving the fractional order ZIKV system.



(A) Fitness(1). (B) EHs(1).

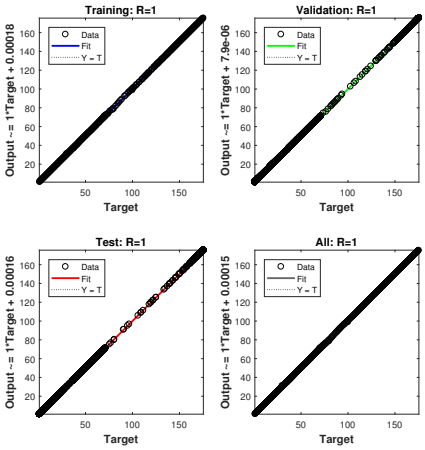
(C) Fitness(2). (D) EHs(2).

(E) Fitness(3). (F) EHs(3).

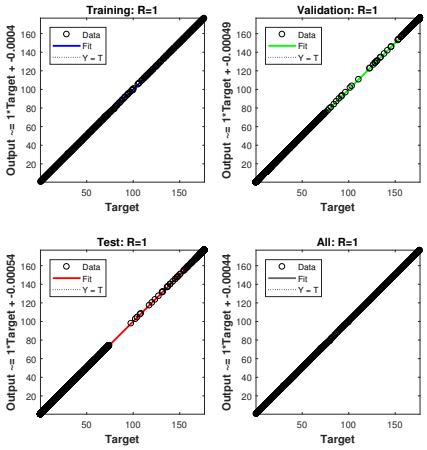
(G) Fitness(4). (H) EHs(4).

FIGURE 5. Valuations of the results and EHs of the fractional order ZIKV model.

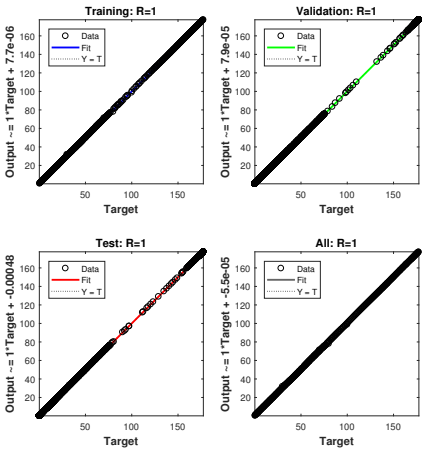
$$
\begin{aligned}
D_t^{0.95} S_h &= (1-p)d_1 - a\lambda m S_h I_v - \theta S_h + n\xi I_h - d_1 S_h, \quad S_h(0) = 100,\\
D_t^{0.95} S_{h_s} &= pd_1 + \theta S_h - a\lambda(1+\delta\lambda^{'}) m S_{h_s} I_v + (1-n)\xi I_h - d_1 S_{h_s}, \quad S_{h_s}(0) = 70,\\
D_t^{0.95} I_h &= a\lambda m S_h I_v + a\lambda m(1+\delta\lambda^{'}) S_{h_s} I_v - (d_1+\phi+\xi) I_h, \quad I_h(0) = 20,\\
D_t^{0.95} S_v &= d_2 - a\beta S_v I_h - d_2 S_v, \quad S_v(0) = 80,\\
D_t^{0.95} I_v &= a\beta S_v I_h - d_2 I_v, \quad I_v(0) = 30.
\end{aligned}
\tag{4.4}
$$



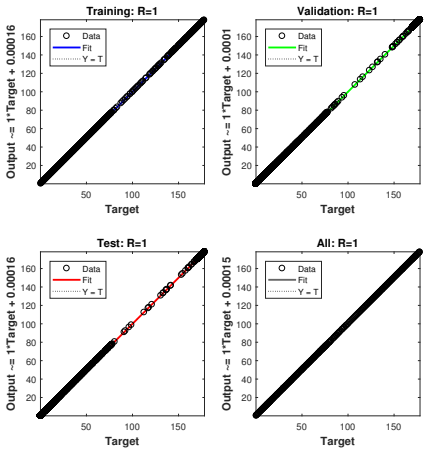
(A) Regression(1).



(B) Regression(2).



(C) Regression(3).



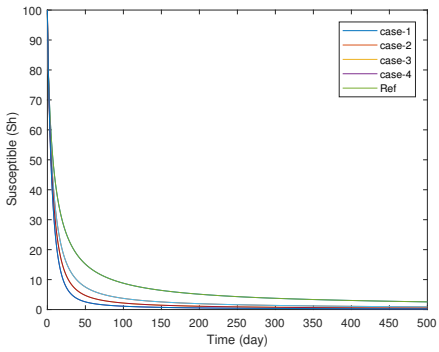
(D) Regression(4).

FIGURE 6. Regression measures for the fractional order ZIKV model.

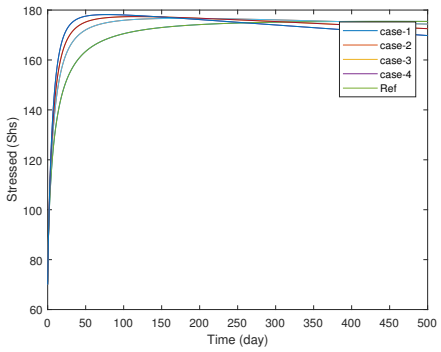
TABLE 3. LMBNNs performances for each case of the fractional-order ZIKV model.

Variant	Validation(MSE)	Performance(MSE)	Gradient	Mu	Iteration	Time(sec)
1	0.00069236	0.000716	0.094374	1×10^{-06}	688	15
2	0.00064752	0.000432	0.062114	1×10^{-06}	1000	21
3	0.00060933	0.00118	0.18257	1×10^{-05}	542	11
4	4.51×10^{-5}	4.90×10^{-5}	0.11369	1×10^{-07}	778	16

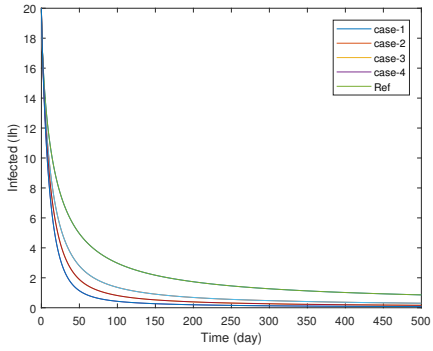
The successful performances made possible by the stochastic structure of LMBNNs (see Figure 2 and Figure 3) are explored with inputs $t \in [0, 500]$ for the ZIKV model (2.1) with 10 neurons organized using the 70% of the training statistics are picked, whereas 50% are chosen for the validation and testing processes. Figures 4-8 display mathematical simulations of the fractional order ZIKV model using the computation outcomes of the LMBNNs.



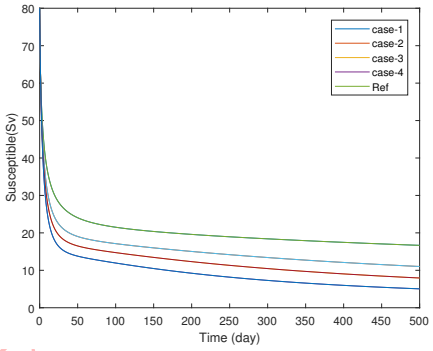
(A) Outcomes for $S_h(t)$.



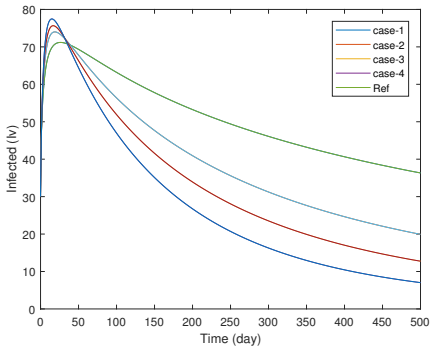
(B) Outcomes for $S_{h_s}(t)$.



(C) Outcomes for $I_h(t)$.



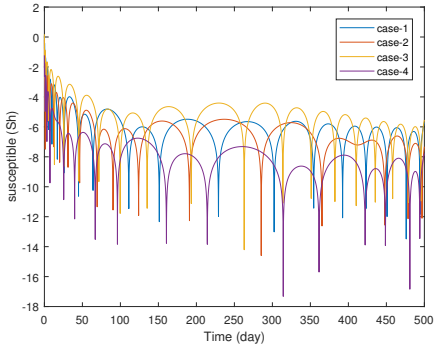
(D) Outcomes for $S_v(t)$.



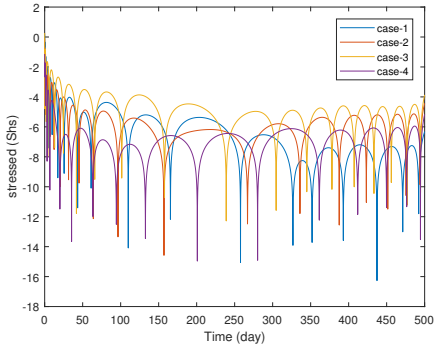
(E) Outcomes for $I_v(t)$.

FIGURE 7. Assessment of the outcomes through the LMBNNs for solving the fractional-order ZIKV model.

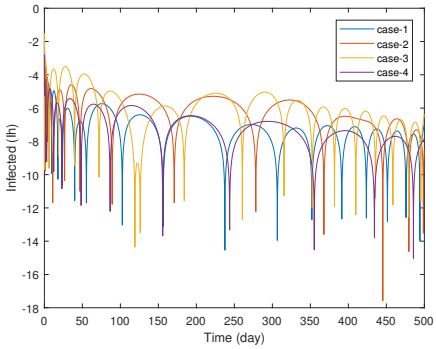
The MSE performance for the fractional order ZIKV model is shown in Figure 4. The best performances values of the fractional order ZIKV model have been computed for FO cases $1, 2, 3$ and 4 are 6.9236×10^{-4}, 6.4752×10^{-4}, 6.0933×10^{-4} and 4.51×10^{-5} with epochs 688, 1000, 542 and 778. The most effective form to test, train, and validate for the proposed fractional order ZIKV model is also depicted in Figures 4(A)-4(H). The values of the gradient are assessed 9.4374×10^{-2}, 6.2114×10^{-2}, 1.8257×10^{-1} and 1.1369×10^{-1} for 1st, 2nd, 3rd and 4th case. The fitness of acquired outcomes and the error histogram (EHs) efficiency for the fractional order ZIKV model via LMBNNs



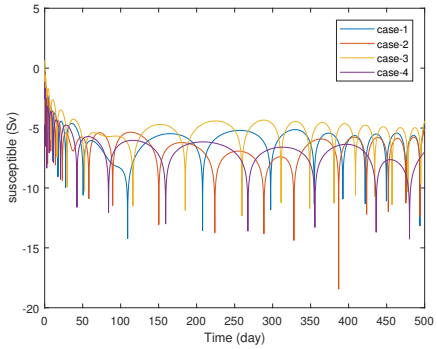
(A) AE for $S_h(t)$.



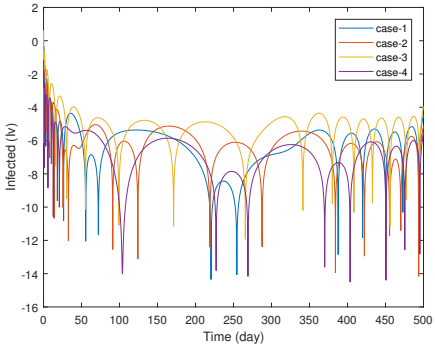
(B) AE for $S_{h_s}(t)$.



(C) AE for $I_h(t)$.



(D) AE for $S_v(t)$.



(E) AE for $I_v(t)$.

FIGURE 8. AE results using LMBNNs for addressing the fractional-order ZIKV model.

are shown in Figure 5. The EHs measures for of the fractional order ZIKV model are computed as -2.967×10^{-2}, -1.928×10^{-2}, -4.514×10^{-2} and -1.551×10^{-2}.

The regression measures utilizing the LMBNNs for the fractional order ZIKV model that are based on the computational approach are presented in Figure 6. Designate the value for correlation values 1 that suggest that the model is optimal to each variant of the fractional order ZIKV model. The procedure for testing, validating, and training describes how accurate the methodology is to solve the fractional type of ZIKV model. The MSE values for the fractional order ZIKV model are calculated using the stochastic technique in Table 3. Results comparison and

absolute error (AE) values for solving the fractional order ZIKV model are shown in Figure 7 and Figure 8. The obtained outcomes indicates the efficiency of the stochastic framework. Figure 8 demonstrates the results of the AE's applying the proposed approach. The AE values for the susceptible (S_h) category are shown in Figure 8(A), where the values for the first, second, third and fourth cases are around 10^{-1} to 10^{-13}, 10^{-1} to 10^{-15}, 10^{0} to 10^{-14} and 10^{-1} to 10^{-17}. For the first, second, third, and fourth cases, the AE for the class stressed (S_{h_s}) is shown in Figure 8(B) to be approximately 10^{0} to 10^{-16}, 10^{-1} to 10^{-13}, 10^{0} to 10^{-12} and 10^{-1} to 10^{-15}. The AE for infected (I_h) has been carried out in Figure 8(C) approximately between 10^{-2} to 10^{-15}, 10^{-3} to 10^{-18}, 10^{-1} to 10^{-14} and 10^{-3} to 10^{-15}. Figure 8(D) presents the susceptible (S_v) AE values performances, which are obtained around 10^{0} to 10^{-14}, 10^{-2} to 10^{-18}, 10^{0} to 10^{-12} and 10^{-1} to 10^{-14}. The calculated AE for the last class of infected (I_v) is 10^{0} to 10^{-14}, 10^{-2} to 10^{-14}, 10^{1} to 10^{-11} and 10^{-1} to 10^{-14}, see Figure 8(E). The correctness of the ANN stochastic process is displayed by the computed AE measures for the proposed ZIKV model (2.1) with Caputo fractional derivative.

5. Conclusions

The goal of this article is to provide a computation context consisting of stochastic LMBNNs in order to give numerical computations of the fractional order ZIKV model. Fractional order studies have been proposed for attaining more accurate results of the ZIKV as compared to integer order. For each ZIKV model category, the numerical simulations have been displayed by using the FO derivatives to solve the four different variations. For the mathematical ZIKV model, the data selection process is carried out as follows: 70% for training and 15% for certification and testing. Throughout the investigation, the fractional order mathematical ZIKV system is solved using 10 neurons. A thorough study has been conducted to examine regression analysis, correlation, MSE, EHs, and information about STs in order to evaluate the proficiency and accuracy of the suggested computing framework. With the objective to slove the fractional order mathematical ZIKV model, the AE was executed in a good manner. The numerical results demonstrate the validity of the stochastic LMBNNs computing framework. Furthermore, the performance is shown to verify the reliability of the scheme. This study offers useful data for future investigations and preventative actions to stop the spread of the Zika virus worldwide. The fractional-order model could be expanded in future studies to include environmental variables and spatial dynamics that affect Zika virus transmission. The predicted accuracy and robustness of the model may be improved by incorporating real-time data from several locations. Examining the effects of interventions like vaccination plans or vector control techniques within the fractional-order framework would shed light on successful public health initiatives to stop the spread of the Zika virus.

Uncorrected Proof

Acknowledgments

The authors would like to express their gratitude to the referees for their constructive and valuable suggestions.

References

[1] A. I. Abushouk, A. Negida, and H. Ahmed, *An updated review of zika virus*, Journal of Clinical Virology, *84* (2016), 53–58.

[2] F. Ahmadkhanpour, H. Kheiri, N. Azarmir, and F. Modarres Khiyabani, *Solving initial value problems using multilayer perceptron artificial neural networks*, Computational Methods for Differential Equations, *13* (2024), 13–24.

[3] A. Ali, Q. Iqbal, J. K. K. Asamoah, and S. Islam, *Mathematical modeling for the transmission potential of zika virus with optimal control strategies*, The European Physical Journal Plus, *137* (2022), 146.

[4] M. Ali, F. E. Guma, A. Qazza, R. Saadeh, N. E. Alsubaie, M. Althubyani, and M. A. Abdoon, *Stochastic modeling of influenza transmission: Insights into disease dynamics and epidemic management*, Partial Differential Equations in Applied Mathematics, *11* (2024), 100886.

[5] M. M. Al-Jebouri, *Modellings of infectious diseases and cancers under wars and pollution impacts in iraq with reference to a novel mathematical model and literature review*, Open Journal of Pathology, *13* (2023), 126–139.

[6] A. Alshehri and M. El Hajji, *Mathematical study for zika virus transmission with general incidence rate*, AIMS Math, *7* (2022), 7117–7142.

[7] S. Alyobi and R. Jan, *Qualitative and quantitative analysis of fractional dynamics of infectious diseases with control measures*, Fractal and Fractional, *7* (2023), 400.
[8] E. O. Alzahrani, W. Ahmad, M. A. Khan, and S. J. Malebary, *Optimal control strategies of zika virus model with mutant*, Communications in Nonlinear Science and Numerical Simulation, *93* (2021), 105532.
[9] L. C. Aulsebrook, B. B. Wong, and M. D. Hall, *Can pharmaceutical pollution alter the spread of infectious disease? a case study using fluoxetine*, Philosophical Transactions of the Royal Society B, *378* (2023), 20220010.
[10] S. K. Biswas, U. Ghosh, and S. Sarkar, *Mathematical model of zika virus dynamics with vector control and sensitivity analysis*, Infectious Disease Modelling, *5* (2020), 23–41.
[11] I. I. Bogoch, O. J. Brady, M. U. Kraemer, M. German, M. I. Creatore, M. A. Kulkarni, J. S. Brownstein, S. R. Mekaru, S. I. Hay, E. Groot, A. Watts, and K. Khan, *Anticipating the international spread of zika virus from brazil*, The Lancet, *387* (2016), 335–336.
[12] E. Bonyah and K. O. Okosun, *Mathematical modeling of zika virus*, Asian Pacific Journal of Tropical Disease, *6* (2016), 673–679.
[13] H. Dadashzadeh, G. Ahmadi, Y. Edrisi Tabrizi, and B. Rezaei, *Flexible fractional wavelet neural network for non-linear system identification*, Computational Methods for Differential Equations, (2025).
[14] K. Diethelm, *A fractional calculus based model for the simulation of an outbreak of dengue fever*, Nonlinear Dynamics, *71* (2013), 613–619.
[15] K. Diethelm and N. Ford, *Analysis of fractional differential equations*, Journal of Mathematical Analysis and Applications, *265*(2) (2002), 229–248.
[16] N. Goswami and B. Shanmukha, *A mathematical analysis of zika virus transmission with optimal control strategies*, Computational Methods for Differential Equations, *9* (2021), 117–145.
[17] N. K. Goswami, S. Olaniyi, S. F. Abimbade, and F. M. Chuma, *A mathematical model for investigating the effect of media awareness programs on the spread of covid-19 with optimal control*, Healthcare Analytics, *5* (2024), 100300.
[18] S. He, S. Tang, Q. Zhang, L. Rong, and R. A. Cheke, *Modelling optimal control of air pollution to reduce respiratory diseases*, Applied Mathematics and Computation, *458* (2023), 128223.
[19] H. W. Hethcote, *The mathematics of infectious diseases*, SIAM review, *42* (2000), 599–653.
[20] H.-F. Huo, T. Fu, and H. Xiang, *Dynamics and optimal control of a zika model with sexual and vertical transmissions*, Math. Biosci. Eng., *20* (2023), 8279–8304.
[21] A. Jan, S. Boulaaras, F. A. Abdullah, and R. Jan, *Dynamical analysis, infections in plants, and preventive policies utilizing the theory of fractional calculus*, The European Physical Journal Special Topics, *232* (2023), 2497–2512.
[22] R. Jan, S. Boulaaras, M. Jawad, and K. Rajagopal, *Effect of virotherapy treatment on the dynamics of tumor growth through fractional calculus*, Transactions of the Institute of Measurement and Control, *45* (2023), 2981–2996.
[23] S. A. Jose, R. Raja, B. Omede, R. P. Agarwal, J. Alzabut, J. Cao, and V. Balas, *Mathematical modeling on co-infection: Transmission dynamics of zika virus and dengue fever*, Nonlinear Dynamics, *111* (2023), 4879–4914.
[24] H. Khan, W. F. Alfwzan, J. Alzabut, D. Almutairi, M. A. Azim, and R. Thinakaran, *Artificial intelligence and neural networking for an analysis of fractal-fractional zika virus model*, FRACTALS, *33* (2025), 1–18.
[25] I. Khan, M. A. Z. Raja, M. Shoaib, P. Kumam, H. Alrabaiah, Z. Shah, and S. Islam, *Design of neural network with levenberg-marquardt and bayesian regularization backpropagation for solving pantograph delay differential equations*, IEEE Access, *8* (2020), 137918–137933.
[26] S. Kumar, S. Sharma, A. Kashyap, N. Kumari, and R. P. Agarwal, *Modelling the effect of environmental pollution on zika outbreak: a case study of brazil*, Discrete and Continuous Dynamical Systems-S, *18*(5) (2025), 1132–1158.
[27] K. D. Lafferty and R. D. Holt, *How should environmental stress affect the population dynamics of disease?*, Ecology Letters, *6* (2003), 654–664.
[28] S. Liu, Z. Luan, S. Kabanikhin, S. Strijhak, and Y. Zhang, *Solving a type of nonlinear schro dinger equations using a physically informed neural network and tuning the adaptive activation function*, TWMS Journal of Pure and Applied Mathematics, *15* (2024), 203–227.

Uncorrected Proof

[29] F. Macnamara, *Zika virus: a report on three cases of human infection during an epidemic of jaundice in nigeria*, Transactions of the royal society of tropical medicine and hygiene, *48* (1954), 139–145.
[30] P. G. Madueme and F. Chirove, *A systematic review of mathematical models of lassa fever*, Mathematical Biosciences, *374* (2024), 109227.
[31] T. Magalhaes, B. D. Foy, E. T. Marques, G. D. Ebel, and J. Weger-Lucarelli, *Mosquito-borne and sexual transmission of zika virus: Recent developments and future directions*, Virus Research, *254* (2018), 1–9.
[32] M. Mullai, G. M. Kumar, G. Rajchakit, and G. Vetrivel, *Mathematical modelling on the transmission dynamics of zika virus*, International Journal on Robotics, Automation and Sciences, *5* (2023), 79–84.
[33] S. Naz, M. A. Z. Raja, A. Kausar, A. Zameer, A. Mehmood, and M. Shoaib, *Dynamics of nonlinear cantilever piezoelectric–mechanical system: An intelligent computational approach*, Mathematics and Computers in Simulation, *196* (2022), 88–113.
[34] B. I. Omede, B. Bolaji, O. J. Peter, A. A. Ibrahim, and F. A. Oguntolu, *Mathematical analysis on the vertical and horizontal transmission dynamics of hiv and zika virus co-infection*, Franklin Open, *6* (2024), 100064.
[35] R. Prasad, K. Kumar, and R. Dohare, *Caputo fractional order derivative model of zika virus transmission dynamics*, J. Math. Comput. Sci, *28* (2023), 145–157.
[36] M. Rahman, K. Bekele-Maxwell, L. L. Cates, H. Banks, and N. K. Vaidya, *Modeling zika virus transmission dynamics: parameter estimates, disease characteristics, and prevention*, Scientific reports, *9* (2019), 10575.
[37] M. A. Z. Raja, M. Shoaib, S. Hussain, K. S. Nisar, and S. Islam, *Computational intelligence of levenbergmarquardt backpropagation neural networks to study thermal radiation and hall effects on boundary layer flow past a stretching sheet*, International Communications in Heat and Mass Transfer, *130* (2022), 105799.
[38] S. Rezapour, H. Mohammadi, and A. Jajarmi, *A new mathematical model for zika virus transmission*, Advances in difference equations, *2020* (2020), 1–15.
[39] Z. Sabir, S. A. Bhat, M. A. Z. Raja, and S. E. Alhazmi, *A swarming neural network computing approach to solve the zika virus model*, Engineering Applications of Artificial Intelligence, *126* (2023), 106924.
[40] Z. Sabir, T. Botmart, M. A. Z. Raja, W. weera, R. Sadat, M. R. Ali, A. A. Alsulami, and A. Alghamdi, *Artificial neural network scheme to solve the nonlinear influenza disease model*, Biomedical Signal Processing and Control, *75* (2022), 103594.
[41] Z. Sabir, R. Sadat, M. R. Ali, S. B. Said, and M. Azhar, *A numerical performance of the novel fractional water pollution model through the levenberg-marquardt backpropagation method*, Arabian Journal of Chemistry, *16* (2023), 104493.
[42] Z. Sabir, S. B. Said, and Q. Al-Mdallal, *A fractional order numerical study for the influenza disease mathematical model*, Alexandria Engineering Journal, *65* (2023), 615–626.
[43] A. M. Salman and M. H. Mohd, *Sustainable covid-19 control measures: A mathematical modelling study*, Journal of Sustainability Science and Management, *19* (2024), 25–35.
[44] Samreen, S. Ullah, R. Nawaz, S. A. AlQahtani, S. Li, and A. M. Hassan, *A mathematical study unfolding the transmission and control of deadly nipah virus infection under optimized preventive measures: New insights using fractional calculus*, Results in Physics, *51* (2023), 106629.
[45] L. Schuler-Faccini, *Possible association between zika virus infection and microcephaly—brazil, 2015*, MMWR. Morbidity and mortality weekly report, *65* (2016).
[46] Z. Shah, M. Raja, Y.-M. Chu, W. Khan, S. Abbas, M. Shoaib, and M. Irfan, *Computational intelligence of levenberg-marquardt backpropagation neural networks to study the dynamics of expanding/contracting cylinder for cross magneto-nanofluid flow model*, Physica Scripta, *96* (2021), 055219.
[47] S. Sharma and N. Kumari, *Dynamics of a waterborne pathogen model under the influence of environmental pollution*, Applied Mathematics and Computation, *346* (2019), 219–243.
[48] N. Sharma, R. Singh, J. Singh, and O. Castillo, *Modeling assumptions, optimal control strategies and mitigation through vaccination to zika virus*, Chaos, Solitons & Fractals, *150* (2021), 111137.
[49] A. K. Srivastav, J. Yang, X. Luo, and M. Ghosh, *Spread of zika virus disease on complex network—a mathematical study*, Mathematics and Computers in Simulation, *157* (2019), 15–38.

Uncorrected Proof

[50] S. Suantai, Z. Sabir, M. A. Z. Raja, and W. Cholamjiak, *Numerical computation of seir model for the zika virus spreading*, Computers, Materials & Continua, *75*(1) (2023), 2155–2170.
[51] P. Suparit, A. Wiratsudakul, and C. Modchang, *A mathematical model for zika virus transmission dynamics with a time-dependent mosquito biting rate*, Theoretical Biology and Medical Modelling, *15* (2018), 1–11.
[52] D. Taylor, *Mathematical model of zika virus transmission and control measures*, The North Carolina Journal of Mathematics and Statistics, *7* (2021), 1–12.
[53] B. Wahid, A. Ali, S. Rafique, and M. Idrees, *Zika: As an emergent epidemic*, Asian Pacific journal of tropical medicine, *9* (2016), 723–729.
[54] A. Wiratsudakul, P. Suparit, and C. Modchang, *Dynamics of zika virus outbreaks: an overview of mathematical modeling approaches*, PeerJ, *6* (2018), e4526.
[55] Z. Yue, Y. Li, and F. M. Yusof, *Dynamic analysis and optimal control of zika virus transmission with immigration*, AIMS Math, *8* (2023), 21893–21913.
[56] Z. U. A. Zafar, M. A. Khan, M. Inc, A. Akgu¨l, M. Asiri, and M. B. Riaz, *The analysis of a new fractional model to the zika virus infection with mutant*, Heliyon, *10* (2024), e23390.

Uncorrected Proof